# Group Formation of Autonomous Underwater Vehicles that Optimizes Energetic Efficiency in Cruising

Gen Li, Ramiro Godoy-Diana, Lei Duan, Benjamin Thiria

# Group Formation of Autonomous Underwater Vehicles that Optimizes Energetic Efficiency in Cruising

Gen Li
Center for Mathematical Science and Advanced Technology
Japan Agency for Marine-Earth Science and Technology
Yokohama, Japan
ligen@jamstec.go.jp

Lei Duan
School of Naval Architecture, Ocean and Civil Engineering
Shanghai Jiao Tong University
Shanghai, China
leiduan@sjtu.edu.cn

Ramiro Godoy-Diana
Laboratoire de Physique et Mécanique des Milieux Hétérogènes (PMMH), CNRS UMR 7636,
ESPCI Paris—PSL University, Sorbonne Université, Université de Paris
Paris, France
ramiro@pmmh.espci.fr

Benjamin Thiria
Laboratoire de Physique et Mécanique des Milieux Hétérogènes (PMMH), CNRS UMR 7636,
ESPCI Paris—PSL University, Sorbonne Université, Université de Paris
Paris, France
bthiria@pmmh.espci.fr

***Abstract*—When AUVs cruise in group, they interact with each other and their energetic efficiency will be influenced. The hydrodynamic interaction among individuals in an AUV group is complex. This challenging hydrodynamic problem is solved by a hybrid, multi-level numerical approach, which consists of individual- and group-level solutions. In the individual-level simulation, based on commercial software and a turbulence model, a full-scale AUV model with realistic propeller morphology is simulated. The result is then input as source information for the group-level solution based on an analytical potential-flow model. This allows us to investigate equilibrium formations for groups of AUVs and evaluate the perspective of energy consumption through their far-field interference. The optimization results suggest that the average energetic consumption of the group may be minimized when leader and follower AUVs stay in a diagonal pattern (i.e. a follower AUV is laterally behind a leader AUV). The AUVs are required to limit their lateral separation distance to maintain the energy saving effect. Our results reveal that, like animals swimming and flying in groups, Autonomous Underwater Vehicles may also adopt specific group formations to optimize energetic efficiency.**

***Keywords—Computational Fluid Dynamics, Autonomous Underwater Vehicle (AUV), energy-saving, underwater robot group, optimization, group formation***

## I. INTRODUCTION

Autonomous Underwater Vehicles (AUVs) are pioneers for humans in ocean exploration. Present-day AUVs are particularly useful as unmanned survey platforms, carrying sensor payloads along pre-programmed trajectories to gather data for a variety of applications [1]. Although in previous decades AUVs were basically operated alone, as more AUVs are brought into operation and AUV missions become large-scaled and complex, understanding the group behavior of AUVs will become necessary (Fig. 1(A) and (B)). For example, as a project already in the process of implementation in Japan, the Japan Agency for Marine-Earth Science and Technology (JAMSTEC) is developing and field-testing a multi-AUV operation ddedicated to the survey of marine resources [2]. Regarding the AUV group operation, most existing studies focus on the communication, planning and navigation algorithm/systems (e.g. [3]–[8]). Nevertheless, the AUV group operation should also be examined from a fluid dynamic perspective. A propelling AUV can generate flow surrounding its hull structure, as well as a wake behind its propeller. Through these flow features, when AUVs cruise together, they will interact with each other. The energetic efficiency and stability of AUVs will be influenced (Fig. 1(C)).

On the other hand, in nature, we can find that swimming and flying animals usually improve their energetic efficiency by moving together with specific group formations [9], [10]. Inspired by these animal group swimming and flying mechanisms, it is worth to examine if AUVs can adopt specific group formations to optimize their energetic efficiency.

The hydrodynamic interaction among individuals in an AUV group is complex. An AUV usually possesses a meter-level body-length, corresponding to Reynolds number (Re) of the order of $10^6$ to $10^8$ [11]. Turbulent flow must be considered in the investigation of AUV hydrodynamics, which however requires much computational time and resources during a numerical solution process. Such computational cost may be afforded in the investigation of a single AUV's hydrodynamics, however, for a group formed by $N$ individuals, the number of

G.L. is funded by the Japan Society for the Promotion of Science (Grant No. 20K14978).

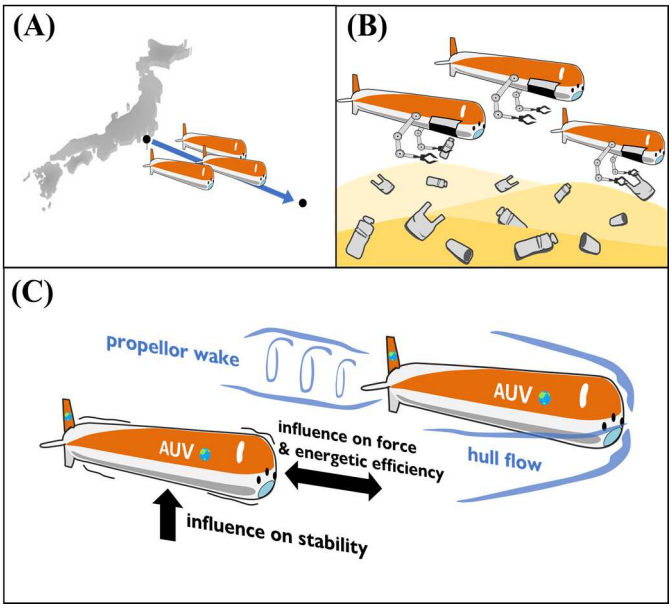


Fig. 1. AUV group operation scenarios and hydrodyanmic interactions. (A) AUV group operation scenario: AUVs moving to a mission site in group. (B) AUV group operation scenario: AUVs cleaning seabottom garbages in group. (C) When AUVs cruise in group, hydrodynamic interaction occours between individuals.

degrees of freedom is 3*N*-3. As *N* increases, the computational cost will eventually become unaffordable.

In this study, this challenging hydrodynamic problem is solved by a hybrid, multi-level numerical approach. This study predicts an optimal formation of a minimal AUV group, which may inspire further optimization work on a larger scale AUV group, and benefit our future AUV-group-based exploration and development in ocean.

## II. Materials and Methods

The hybrid, multi-level numerical approach used in this study consists of individual- and group-level solutions. In the individual level, computational fluid dynamic (CFD) simulations with turbulence model are implemented to obtain flow field and propulsive performance of a single cruising AUV. The result is then input as source information for the group-level solution. Unsteady flow field is time-averaged into a steady axisymmetric flow. The velocity field far from an individual AUV is approximated by the velocity field of a vortex ring and a momentumless wake. The group-level simulation is based on an analytical potential-flow model. Simulations on an individual AUV

The CFD simulation on an individual AUV is based on commercial software Siemens Simcenter STAR-CCM+ 2020.1 and Reynolds averaged Navier-Stokes (RANS) turbulence model, a 1:1 full-scale AUV model with realistic propellor morphology is simulated. The CFD software and turbulent model have been validated in a study on rotational wind blades [12]. The hardware used for simulation is a workstation with AMD EPYC 7502P processor (32 cores, 64 threads, 2.5-3.35 GHz) and 256G memory at 2933 MHz. The simulation setting parameters are summed up in Table 1.

Table 1. Individual AUV simulation parameters

| | |
|---|---|
| AUV model dimension | Length: 3.4 m<br>Diameter: 0.35 m<br>1:1 scale |
| Center of mass setting | 1.64 m downstream from the AUV nose |
| Turbulence model | SST k-_ model |
| Computational domain | Length: 12 m<br>Diameter: 6 m |
| Time step | 0.0015625 s |
| Inner iterations | 10 |

The computational mesh in the individual AUV simulation is demonstrated in Fig. 2. The propeller zone is rotating while the other parts are static regions covered by a Cartesian mesh. For the static mesh, the mesh part at the AUV surface and rear zone are refined (Fig.2(B)). The setting parameters of the static mesh are summed up in Table 2. The rotational propeller zone possesses the highest resolution mesh (Fig.2(C)), and its meshing parameters are summed up in Table 3.

The boundary condition at the frontal surface (Fig.2A) of the computational domain is set as velocity inlet at various value in each case. The rear surface of the computational domain is set as zero-pressure outlet. The side surfaces are set as symmetry boundary.

During the individual-level simulation, we firstly set a cruising propeller rotational speed (set as 320 rpm). Through multiple iterative simulations, cruising speed $U_0$ is determined. At cruising speed $U_0$, the propeller power and the flow field around the AUV are recorded. Furthermore, by conducting further simulations the derivatives of power and flow field with respect to the cruising speed $U_0$ are computed.

Table 2. Static mesh parameters in individual AUV simulation

| | |
|---|---|
| Total mesh grid number | 5.17 million |
| Boundary layers | Thickness: 0.015 m<br>Growth rate: 1.2<br>number of layers: 10 |
| Computational domain | Length: 12 m<br>Diameter: 6 m |
| Maximum Grid size | 0.16 m, isotropous |
| Grid refinement | Near AUV body: 0.01 m<br>Rear part: 0.005 m |

TABLE 3. ROTATIONAL MESH PARAMETERS IN INDIVIDUAL AUV SIMULATION

| | |
|---|---|
| Total mesh grid number | 0.87 million |
| Boundary layers | Thickness: 0.005 m<br>Growth rate: 1.2<br>number of layers: 5 |
| Maximum Grid size | 0.01 m, isotropous |
| Grid refinement | Near blade surface, 0.0025 m.<br>On the blade leading and tailing edges: 0.0005 m |

### A. *Group level anaylsis*

The results obtained by the individual AUV simulation is then input as source information for the group-level solution. Unsteady flow field is time-averaged into a steady axisymmetric flow. The group-level simulation is based on an analytical potential-flow model, we approximate the velocity field far from an individual AUV by the velocity field of a vortex ring [13] and a momentumless wake [14]. This allows us to investigate equilibrium formations for groups of AUVs and evaluate the perspective of energy consumption through their far-field interference.

The circulation $\Gamma$ and the hydrodynamic power $P$ of a swimmer are functions of the local inflow velocity of the surrounding fluid $U$. These functions can be linearized for small deviations of $U$ from some reference velocity $U_0$,

$$\begin{aligned} \Gamma(U) &= \Gamma|_{U_0} + \left.\frac{\partial \Gamma}{\partial U}\right|_{U_0} (U - U_0), \\ P(U) &= P|_{U_0} + \left.\frac{\partial P}{\partial U}\right|_{U_0} (U - U_0), \end{aligned} \tag{1}$$

where the $\Gamma$, $P$ and their derivatives at $U_0$ are evaluated using individual AUV CFD simulations.

The inflow velocity at the location of one arbitrary AUV swimmer is the superposition of $U_0$ and the velocity induced by all companion swimmers. We aim to minimize the normalized average mechanical power expenditure in the group with $3N - 3$ optimization parameters, where $N$ is the number of AUV swimmers in the group.

## III. RESULTS

### A. *Simulation reuslts of an individual AUV*

We set a cruising propeller rotational speed of 320 rpm. Multiple iterative simulations were conducted and approach the equilibrium condition (AUV drag=thrust) until the absolute difference between drag and thrust is less than 0.05N, and the absolute value of force difference ratio (calculated as (drag-thrust)/thrust) is less than 0.3% (see Table 4). Cruising speed $U_0$ was determined as 1.63 m/s, which is defined as the *standard case*. The propeller power of the standard case was recorded (see Table 4 and Fig. 3). The time-sequence flow field around the AUV in the standard case was recorded as well (see Fig. 4(A) and (B)).

Based on the standard case, multiple further simulations were implemented to approach the equilibrium condition at cruising speeds of 90%, 98%, 102% and 110% of the speed of the standard case (see Table 4 and Fig. 3). According to the curve fitting results of Fig.3, around the standard speed of 1.63m/s, AUV speed is linearly proportional to propellor rotational speed; The thrust of the AUV (note that in equilibrium condition thrust equals to drag) is approximately proportional to the square of AUV speed; The power of the AUV is approximately proportional to the cube of AUV speed.

The time-sequence flow field around the AUV in those four derived cases were also recorded.

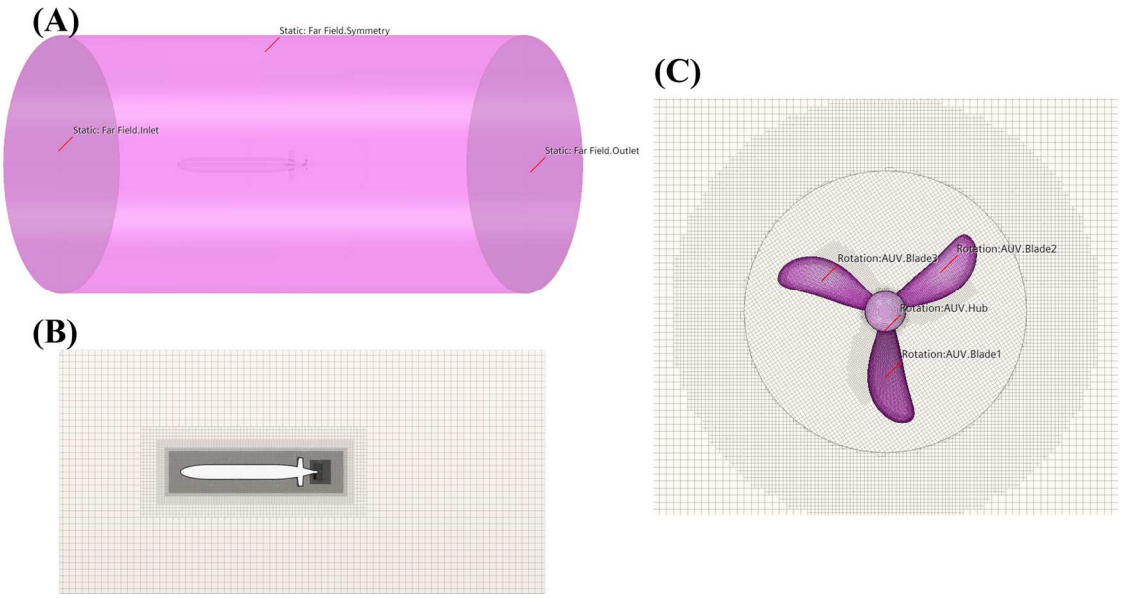


Fig. 2. The computational mesh in the individual AUV simulation. (A) Three-dimensional view of the computational domain. The boundary condition at frontal surface is set as velocity inlet. The rear surface is set as zero-pressure outlet. The side surfaces are set as symmetry boundary. (B). Static mesh, where the mesh part at AUV surface and rear zone are refined. (C) The rotational propellor zone.

TABLE 4. COMPUTATIONAL RESULTS OF INDIVIDUAL AUV PERFORMANCE

| Case | Propellor Rotation (rpm) | Cruising speed (m/s) | Drag (N) | Unbalanced Force (N) | Thrust (N) | propellor power (W) |
|---|---|---|---|---|---|---|
| **90% speed** | 288 | 1.467 | 15.770 | 0.046 | 15.724 | 32.985 |
| **98% speed** | 313.6 | 1.597 | 18.390 | 0.039 | 18.351 | 41.959 |
| **Standard Cruising (100% speed)** | 320 | 1.630 | 19.075 | 0.033 | 19.042 | 44.436 |
| **102% speed** | 326.4 | 1.663 | 19.772 | 0.034 | 19.739 | 46.995 |
| **110% speed** | 352 | 1.793 | 22.680 | 0.029 | 22.651 | 58.211 |

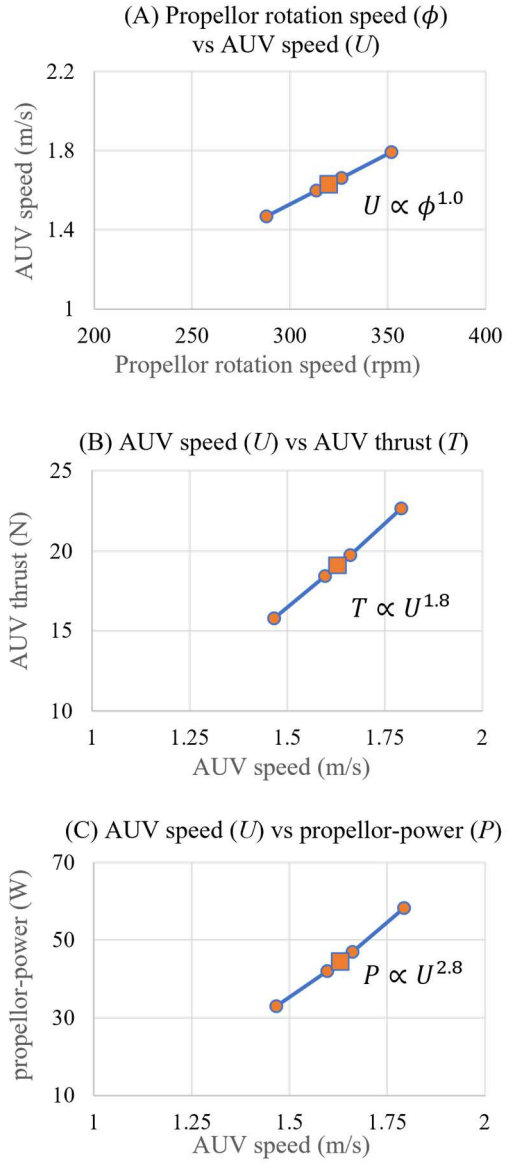


Fig. 3. AUV propulsive performance results in the individual AUV simulation at five various speeds. (A) Propellor rotation speed vs AUV speed. (B) AUV speed vs AUV thrust, while in equilibrium condition thrust equals to drag. (C) AUV speed vs AUV propellor power. Results of the standard case are highlighted by square symbols.

### B. *Group level anaysis results*

The unsteady flow fields of an individual AUV, as demonstrated by Fig. 4(A), were time-averaged and converted into a steady axisymmetric flow, as shown by Fig.4(B). This steady axisymmetric flow is then expressed by a sum of multiple vortex rings with infinitesimally thin cores and a momentumless wake. The resultant flow field after fitting is very similar to the CFD result (Fig. 4(C)), and can be applied in an analytical potential-flow model.

Till here, the information needed by Eq. 1 has been satisfied and we then perform the optimization by the analytical model. We use the CMA-ES genetic optimization algorithm [15]. To accelerate the search, the swimmer coordinates vary with discrete increments that are multiples of $0.01R$ ($R$ is the AUV radius), and sufficient number of iterations were performed to ensure that the objective function of optimization does not change by more than $10^{-4}$ during the last 100 iterations. We obtained optimal group formation for AUV group consisting of 2 individuals (an example shown in Fig.5). The AUVs are required to limit their lateral separation distance to maintain energy saving effect. The optimization results suggest that the average energetic consumption in the group may minimize when leader and follower AUVs stay in a diagonal pattern (i.e. a follower AUV is laterally behind a leader AUV), which is similar to the results reported in a fish group consisting of two individuals [16],[17]. In the case shown by Fig. 5, the AUV group can save approximately 3% power without any sacrifice of their speed. Our results reveal that, like those animals swimming and flying in group, Autonomous Underwater Vehicle may also adopt specific group formation to optimize energetic efficiency.

## IV. CONCLUSION

We developed a hybrid computational approach and obtain optimal formation for AUV group. The CFD simulation on one individual AUV provides many important details about the flow field and propulsive performance of a cruising AUV, while by converting the unsteady flow fields of an individual AUV into time-averaged steady axisymmetric flow and expressed by basal momentumless flow patterns. Optimization on group formation is performed by the analytical model. The AUVs are required to limit their lateral separation distance to maintain energy saving effect. The optimization results suggest that the average energetic consumption in the group may minimize when leader and follower AUVs stay in a diagonal pattern (i.e.

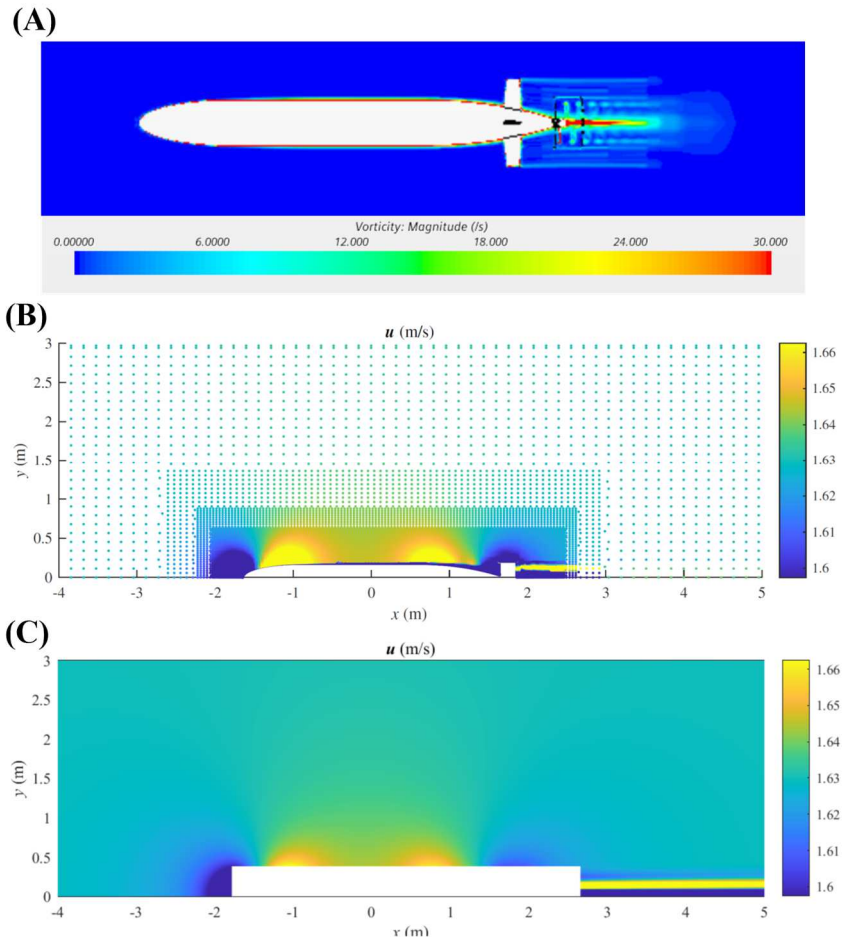


Fig. 4. CFD flow fiield and convertion process. (A) Unsteady flow fields of an individual AUV. (B) Transient flow field data of an individual AUV is time-averaged and converted into a steady axisymmetric flow. (C) The flow field of (B) is then expressed by a sum of multiple vortex rings with infinitesimally thin cores and a momentumless wake. The resultant flow field (C) after fitting is very similar to the CFD result (B) at the regions far from the AUV.

a follower AUV is laterally behind a leader AUV). Our results reveal that, like animals swimming and flying in groups, Autonomous Underwater Vehicle may also adopt specific group formation to optimize energetic efficiency.

## ACKNOWLEDGMENT

We thank Dr. Dmitry Kolomenskiy for his critical advice during the research and the writing of this paper.

## REFERENCES

[1] J. W. Nicholson and A. J. Healey, "The present state of Autonomous Underwater Vehicle (AUV) applications and technologies," *Mar Technol Soc J*, vol. 42, no. 1, pp.44–51, 2008.

[2] Japan Agency for Marine-Earth Science and Technology, "Research and development of multiple AUV operation methods, etc (in Japanese)," jamstec.go.jp. https://www.jamstec.go.jp/sip/enforcement-2/development2-2.html. (accessed Dec. 18, 2022).

[3] Y. Chen, X. Guo, G. Luo, and G. Liu, "A Formation Control Method for AUV Group Under Communication Delay," *Front Bioeng Biotechnol*, vol. 10, p. 848641, 2022.

[4] L. Hongli, W. Hongjian, L. Qing, and Y. Hongfei, "Task allocation of multiple autonomous underwater vehicle system based on multi-objective optimization," in *2016 IEEE International Conference on Mechatronics and Automation,* pp. 2512–2517, 2016.

[5] T. Pang, Y. Song, and D. Zhu, "Task allocation for multi-AUV system under ocean current environment," in *Proceeding - 2021 China Automation Congress,* pp. 4844–4849, 2021.

[6] X. Ma, C. Yanli, G. Bai, and J. Liu, "Multi-AUV Collaborative Operation Based on Time-Varying Navigation Map and Dynamic Grid Model," IEEE Access, vol. 8, pp. 159424–159439, 2020.

[7] N. Sergeenko, A. Scherbatyuk, and F. Dubrovin, "Some algorithms of cooperative AUV navigation with mobile surface beacon," in *OCEANS 2013 MTS/IEEE - San Diego: An Ocean in Common*, pp. 1–6, 2013.

[8] F. Dubrovin, Y. Vaulin, A. Scherbatyuk, D. Scherbatyuk, and A. Rodionov, "Navigation for AUV, Located in the Shadow Area of LBL, during the Group Operations," in *2020 Global Oceans 2020: Singapore - U.S. Gulf Coast*, pp. 1–6, 2020.

[9] P. Alexandre, Y. Clerquin, S. Jiraskova, J. Martin, and H. Neimerskirch, "Energy Saving in Flight Formation," *Nature*, vol. 413, pp. 697–698. 2001.

[10] I. Ashraf, H. Bradshaw, T. T. Ha, J. Halloy, R. Godoy-Diana, and B. Thiria, "Simple phalanx pattern leads to energy saving in cohesive fish schooling," *Proc Natl Acad Sci U S A*, vol. 114, no. 36, pp. 9599–9604, 2017.

[11] K. Mostafapour, N. M. Nouri, and M. Zeinali, "The effects of the Reynolds number on the hydrodynamics characteristics of an AUV," *Journal of Applied Fluid Mechanics*, vol. 11, no. 2, pp. 343–352, 2018.

[12] Y. Fang, G. Li, L. Duan, Z. Han, and Y. Zhao, "Effect of surge motion on rotor aerodynamics and wake characteristics of a floating horizontal-axis wind turbine," *Energy*, vol. 218, p. 119519, 2021.

[13] C. K. Batchelor and G. K. Batchelor, “An introduction to fluid dynamics, ” *Cambridge University Press*, 2000.

[14] V. I. Korobko, V. K. Shashmin and Z. P. Shul'Man, (). “Contribution to the theory of laminar momentumless wakes,” *Fluid Dynamics*, vol. 21, pp.195–199, 1986.

[15] N. Hansen, S. D. Müller, and P. Koumoutsakos, “Reducing the time complexity of the derandomized evolution strategy with covariance matrix adaptation (CMA-ES),” *Evol Comput*, vol. 11, no. 1, pp. 1–18, 2003.

[16] G. Li, D. Kolomenskiy, H. Liu, B. Thiria, and R. Godoy-Diana, “On the energetics and stability of a minimal fish school,” *PLoS One*, vol. 14, no. 8, pp. 1–20, 2019.

[17] G. Li, D. Kolomenskiy, H. Liu, B. Thiria, and R. Godoy-Diana, “On the interference of vorticity and pressure fields of a minimal fish school,” *Journal of Aero Aqua Bio-mechanisms*, vol. 8, no. 1, pp. 27–33, 2019.

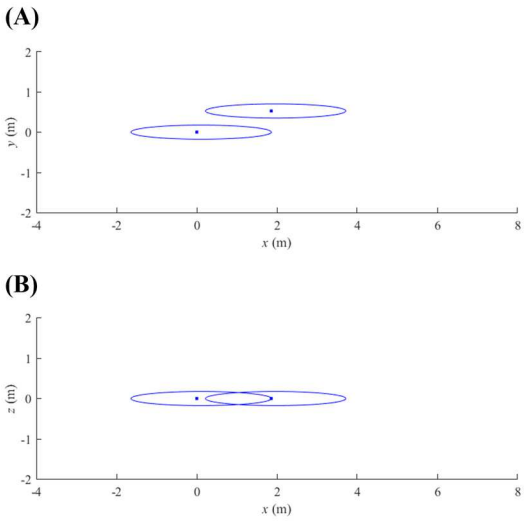


Fig. 5. An example optimal group formation consisting of two individuals, when the minimal allowed lateral-distance between AUVs is set as three times of AUV radious.